Pergamon

Piggyback basin development and thrust belt evolution: structural and palaeostress analyses of Plio-Quaternary basins in the Southern Apennines

J. C. HIPPOLYTE and J. ANGELIER

Département de Géotectonique, Université P. et M. Curie, Boîte 129, 75252 Paris Cédex 05, France

F. ROURE

Institut Français du Pétrole, B.P. 311, 92506 Rueil-Malmaison Cédex, France

and

P. CASERO

Total TEP DE-DBF, Tour Total, Defense 10, 92069 Paris La Defense Cédex 47, France

Abstract—In southern Italy, structural analysis of the intramontane Pliocene–Quaternary terrigenous basins of Sant'Arcangelo and Ofanto shows that they are piggyback basins. The recent uplift of the Southern Apennines provides good conditions for carrying out detailed studies of palaeostresses in relation to structure and sediment accumulation in such piggyback basins. We demonstrate that in the Pleistocene Sant'Arcangelo marine basin, a single N70° compression induced a complex pattern of folds and strike-slip faults. In contrast, the older Pliocene Ofanto basin reveals a polyphase history characterized by successive tilts and palaeostresses according to different compressions. In both basins, compressional stresses are syn-depositional. The geometry of the sedimentary infill of these basins provides information on the thrusting activity in terms of location, geometry and age. We point out that, in addition to sedimentary and structural studies (including interpretation of seismic reflection data), palaeostress analyses provide a valuable tool for deciphering development and evolution of compressional basins in a fold-and-thrust belt.

INTRODUCTION

THE term 'piggyback basin' was proposed by Ori & Friend (1984) for sedimentary basins formed and filled while being carried on active thrust sheets. Some examples have been described in the Northern Apennines (Fig. 1a) where the Plio-Quaternary Po plain basin is documented from seismic and well controls (Pieri 1983, Castellarin & Vai 1986, Ricci Lucchi 1986, Fesce 1987, Zoetemeijer et al. 1992).

In the southern Apennines (Fig. 1b), recent uplift of the mountain chain and of its foredeep, and subsequent erosion, allow direct field observation of marine sediments deposited in Plio-Quaternary intramontane basins. In the past, these basins were interpreted as post-tectonic (Ogniben 1969, Vezzani 1975), or deformed after their deposition (Gars 1983, Patacca & Scandone 1987, Bigi et al. 1992), or related to late distensive tectonics (D'Argenio et al. 1975, Ippolito et al. 1975, Caldara et al. 1988). Based on seismic interpretation, Casero et al. (1988, 1991) and Roure et al. (1988, 1991) interpreted these basins as syn-tectonic compressional piggyback basins.

How did these basins develop within the complex, polyphase history of the mountain belt? Did extensional tectonism occur? To answer these questions, detailed structural analyses combined with palaeostress recon-

structions were carried out in the Sant'Arcangelo and Ofanto basins (Fig. 1b). This approach, combining surface and subsurface studies, enables us to check the hypothesis of their piggyback origin. Further, it allows characterization of the stress regime that prevailed in such basins; the relationships between basin fill and compressional deformation were especially studied.

GEOLOGIC SETTING

The Apenninic chain (Fig. 1) is a Neogene thrust belt, resulting from the deformation of the Apulian continental margin (Haccard et al. 1972, Grandjacquet & Mascle 1978). This arc-shaped chain is associated with a back-arc extensional basin, the Tyrrhenian basin (Fig. 1a) (Boccaletti et al. 1976, Moussat 1983, Kastens et al. 1987). To the south, the subduction of the Ionian oceanic lithosphere is still active in the Calabrian arc where a Wadati–Benioff zone is present (Ritsema 1979, Gasparini et al. 1982, Anderson & Jackson 1987). The Southern Apennines (Fig. 1b) represent an onshore segment of the arc and its structure is well documented by seismic profiles (Mostardini & Merlini 1988, Casero et al. 1988). It results from the tectonic stack of rock units derived from different Mesozoic to Palaeogene sedimentary
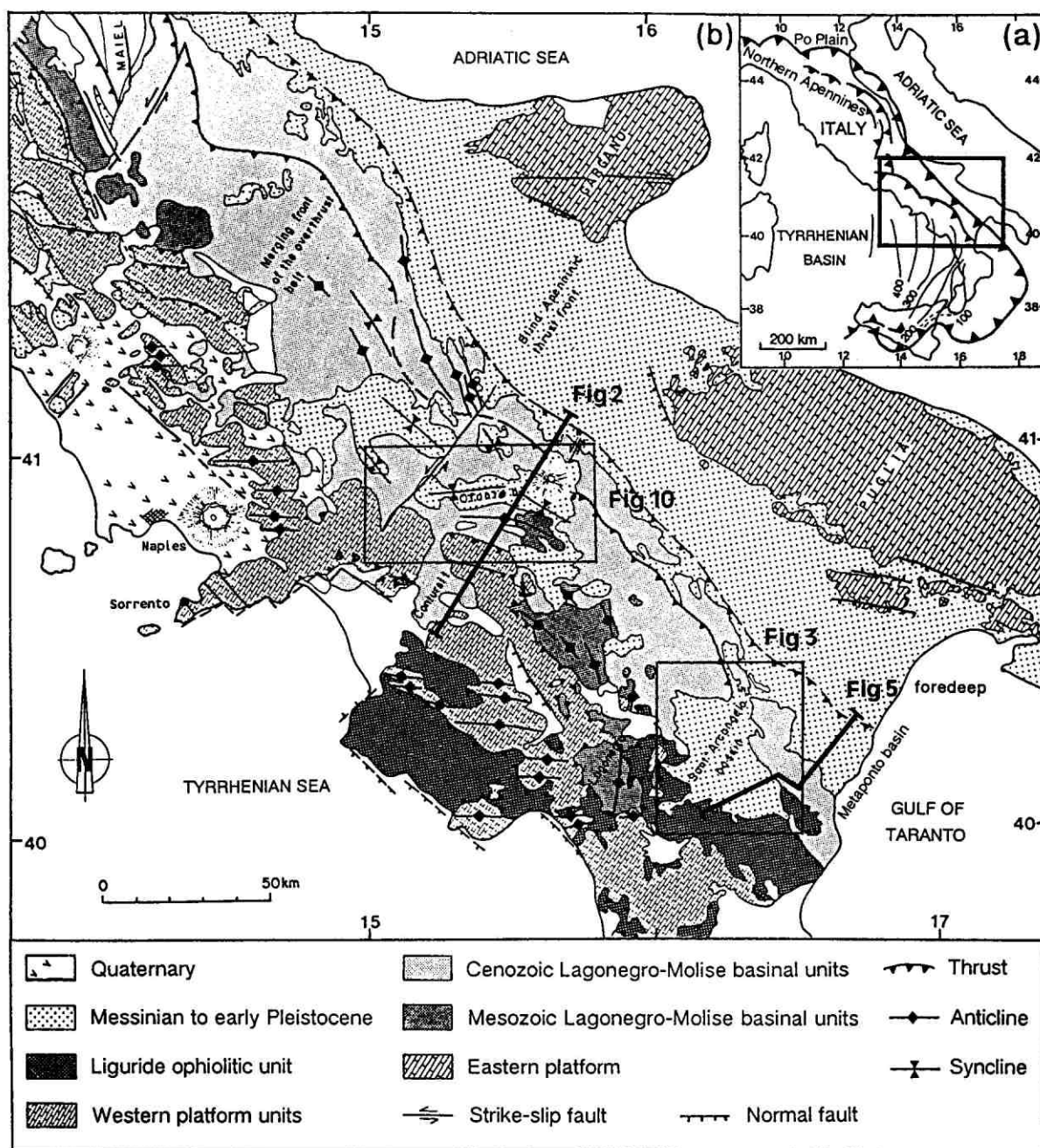
Fig. 1. Structural sketch of the Tyrrhenian arc. (a) Location of the area in Italy (contours show depth of the Benioff zone, in km, after Anderson & Jackson 1987). (b) Southern Apennines, modified from Roure et al. (1991), with fold axes from Ortolani & Torre (1981).

domains, including basins and shelves (Ogniben 1969, D'Argenio et al. 1975, Mostardini & Merlini 1988).

Cross-sections display the superposition of western shelf carbonate units overriding basinal units (Lagonegro–Molise) which in turn lie on the eastern carbonate platform (Casero et al. 1988, Mostardini & Merlini 1988) (Fig. 2). The eastern carbonate platform is also deformed by compression. The most striking structural feature is the presence of an overthrust belt (Casero et al. 1991) which developed in this eastern platform unit beneath the basinal units (Fig. 2). In contrast, along the western side of the belt, near the Tyrrhenian back-arc basin, extension is present, with large normal faults (Fig. 2, left tip). Both Plio-Quaternary marine basins considered in the present paper are located on the top of the basinal thrust units, at the eastern edge of the buried overthrust belt (Fig. 2).

THE SANT'ARCANGELO BASIN

The Sant'Arcangelo Basin, located near the Gulf of Taranto (Fig. 1b) is the most recent onshore Plio-Quaternary marine basin of the Southern Apennines.

Stratigraphy

Due to the recent regional uplift, outcrops of Pleisto-cene marine sediments are now more than 700 m above sea level. The Sant'Arcangelo basin (Fig. 3) is filled by a
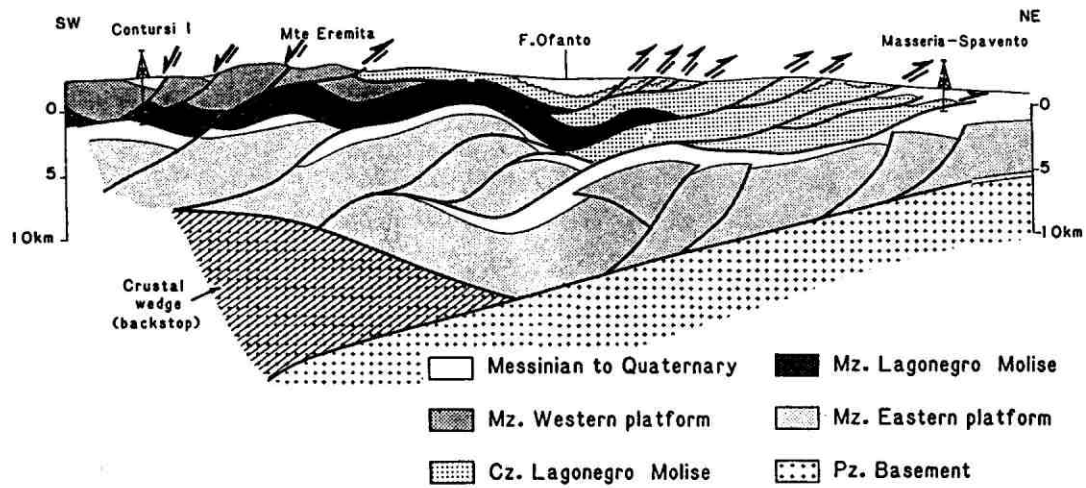
Fig. 2. Cross-section of the southern Apennines (from Casero *et al*. 1991). See location in Fig. 1. (Horizontal scale = vertical scale.)
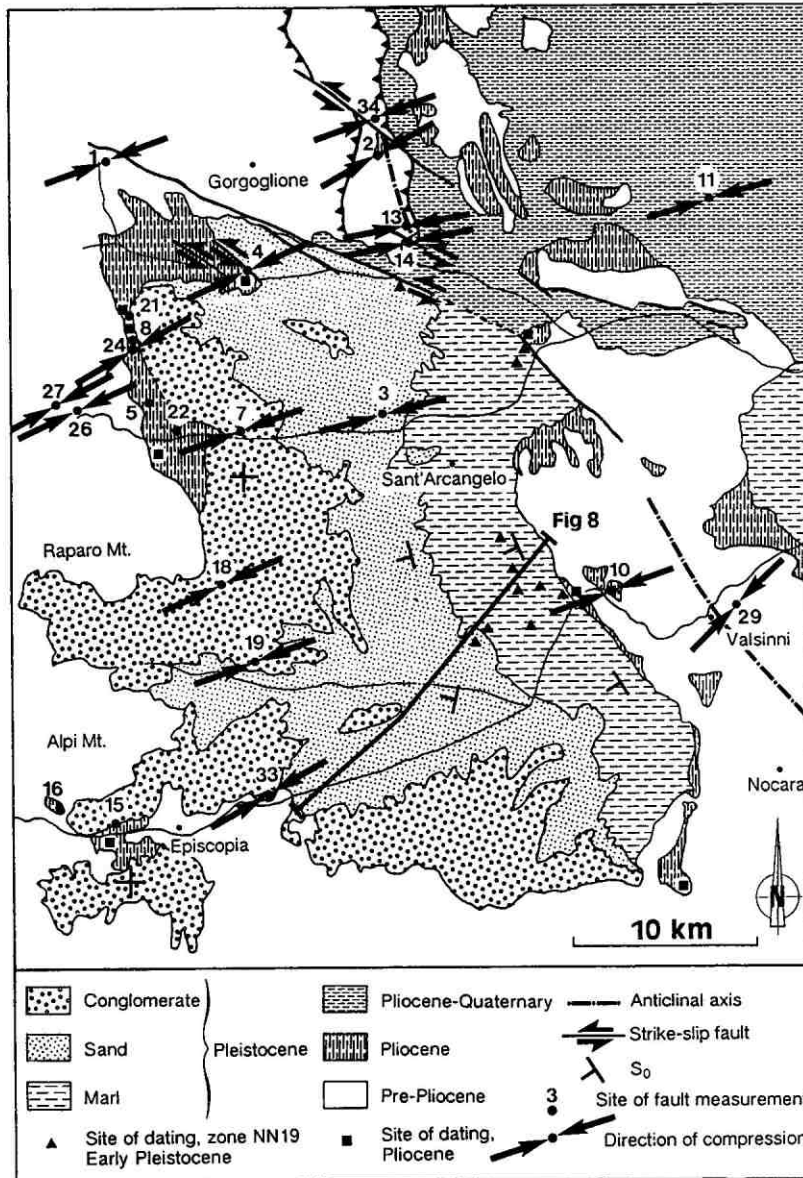

Fig. 3. Geological sketch of the Sant'Arcangelo basin with Pleistocene compression directions (see location in Fig. 1).

thick (more than 3000 m) terrigeneous sequence, which unconformably overlies Pliocene and older rocks (Vezzani 1967). The basin infill presently forms a monocline dipping to the southwest. From bottom to top and from northeast to southwest, blue–grey marly clays, sands and conglomerates belong to a typical regressive depositional sequence showing evolution from marine to littoral, fluviatile and lacustrine deposit environment (Vezzani 1967, Ogniben 1969). We obtained an early Pleistocene age (nannoplankton zone NN19) for the lower clays (presence of *Pseudoemiliania lacunosa* and *Gephyroscapsa oceanica*; sites indicated by triangles in Fig. 3). They are thus younger than the previously assumed late Pliocene–Calabrian age (Vezzani 1967, Ogniben 1969). Considering the occurrence of *Elephas meridionalis* in the upper conglomeratic formation (Vezzani 1967), we consequently attribute the entire basin fill to early Pleistocene age. Beneath the basal unconformity of the Pleistocene, the presence of a Pliocene sequence is confirmed (probably zone NN15, with *Pseudoemiliania lacunosa*, *Helicosphaera sellii*, *Reticulofenestra pseudoumbilica*, *Discoaster surculus*, *D. brouweri*, *D. tamalis*; Fig. 3, squares). The angular unconformity between these two depositional sequences reaches up to 65° (Vezzani 1967).

Structures

Very few normal faults were observed in the Plio-Pleistocene sediments (Bousquet 1973, Gars 1983, Caldara *et al.* 1988) and no large normal fault affects the Pleistocene basin. In contrast, compressional structures are well developed. The eastern part of the basin, near Valsinni (Fig. 3), is bordered by a complex nappe anticline which affects the pre-Pleistocene substratum of the basin. This anticline also deforms the Pleistocene sediments which are locally truncated by a lower–middle Pleistocene marine terrace (Fig. 4). The development of this fold could result from the emplacement of a thrust ramp in the underlying units (borehole interpretation, Gars 1983) during the lower–middle Pleistocene. This structure is summarized in the cross-section of Fig. 5.

Eastward, in the foredeep (Fig. 1b), several boreholes (Ogniben 1969, Balduzzi *et al.* 1982) show the existence of the Metaponto unit, overthrusted above late Pliocene and Pleistocene sediments (Fig. 5).

The northern border of the basin, near Gorgoglione (Fig. 3), strikes parallel to left-lateral strike-slip faults

Fig. 4. Landscape sketch of the eastern flank of the Valsini fold. Calabrian clays are tilted to the northeast and uncomformably overlain by a Pleistocene marine terrace.

visible in the field. One of these faults offsets earlier folds and thrust fronts by about 3 km (Fig. 3, near site 34).

Palaeostresses

A total of 430 fault planes with slickenside lineations were measured in 23 sites, both in and around the basin (Fig. 3). These data allow stress determinations to be made (Table 1), based on fault-slip data analysis (Angelier 1990). This analysis reveals that Pleistocene sediments are affected by a single major compression trending WSW–ENE (Fig. 3 and Table 1, sites 3, 7, 18 and 19). Despite the complexity of the basin, the development of folds and faults was controlled by a surprisingly simple stress field. Figure 3 illustrates this contrast between the complexity of the structural pattern and the homogeneity of the stress trends.

For example, in the central area of the basin (site 3 in Fig. 3), a fold (Fig. 6a) with NNW–SSE-trending axis results from the same WSW–ENE compression which was reconstructed through the analysis of minor fault sets (Fig. 6c and Table 1). In addition, an angular unconformity in the western flank of this anticline (Fig. 6b) shows that folding (due to the WSW–ENE compression) was active during the deposition of the early Pleistocene sediments. Moreover, a strike-slip fault, close to the major fault which bounds the basin to the north (Fig. 3, site 4), also moved consistent with WSW–ENE compression as shown by detailed analyses of fault sets.

This single palaeostress regime affected all the Quaternary deposits, including the uppermost layers of the basin, which remained approximately horizontal (Fig. 3). Pleistocene deposits are affected only by compression trending N70° ($\pm 7°$). We conclude that a compressional regime prevailed during the development of the basin and the formation of the arc-shaped thrust–fold structure limiting the basin in the east (Fig. 3).

Palaeostress was also determined in the Pliocene deposits, beneath the Pleistocene unconformity (Table 1). Two directions of compression (i.e. strictly compressional with σ_3 vertical, or of strike-slip type with σ_2 vertical) are identified (Figs 3 and 7a & b). Their trends are N70° ($\pm 11°$) and N20° ($\pm 22°$). Relative chronologies based on successive slickenside lineations (five observations in sites 13, 24 and 33, Figs 7b & d) indicate that the N70° compression post-dates the N20° one. We therefore ascribe the N70° compression evidenced in the Pliocene sediments, to the syn-depositional N70° Pleistocene compression previously discussed. The N20° compression, pre-dating the N70° Pleistocene compression, and not found in the Pleistocene deposits, is Pliocene in age.

Note that, in addition, some extensional phenomena with scattered trends were identified in Pliocene sediments (Fig. 7c). Their interpretation is ambiguous because they may well correspond to local phenomenon of sliding or compaction of clays rather than to deep-seated extension. However, significant extension along a
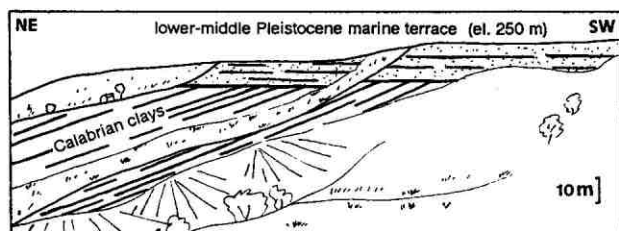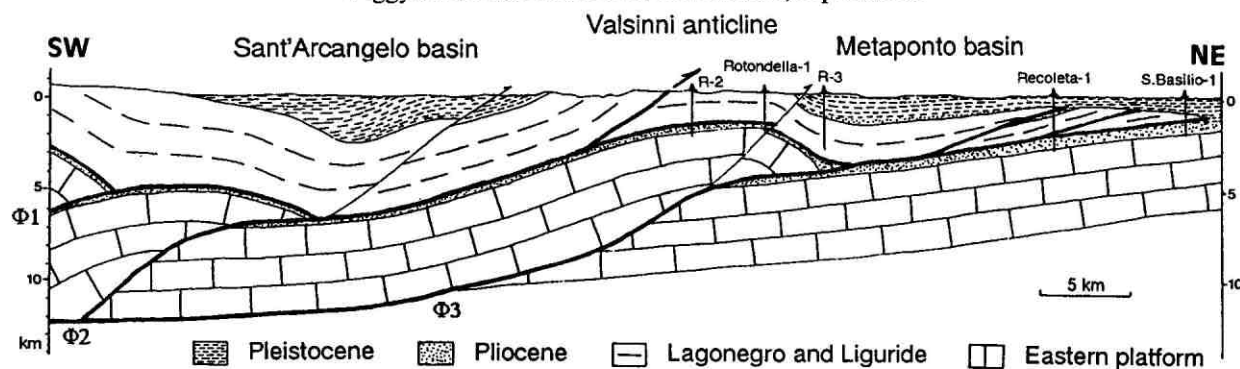
Fig. 5. Interpretative cross-section of the Sant'Arcangelo area (see location in Fig. 1).

WNW–ESE-trend is associated with large normal faults. In site 33, we could observe one of these faults, with associated minor faults and tension gashes (Fig. 7d), sealed by the Pleistocene marine sediments. This extension is Pliocene in age. Its σ_3 axes have the same trend as those of the strike-slip deformation of the ~N20° compression (Fig. 7d), suggesting a phenomenon of permutation of stress axes σ_2 and σ_1 (Angelier & Bergerat 1983): the maximum horizontal stress remains constant in direction, but changes from σ_2 to σ_1. These two states of stress (extension and strike-slip) are contemporaneous on a geological time scale and do not necessarily belong to distinct tectonic events, as pointed out earlier (Hippolyte et al. 1992).

We conclude that, during Pliocene times, the Sant'Arcangelo area was characterized by a WNW–ESE exten-

sion associated with strike-slip deformation so that compressional axes trend N20° (±22°) and extensional ones trend N110° (±37°). Note that south of this area (in Calabria), extension was active with a similar trend, since late Tortonian (Ghisetti 1979, Bousquet et al. 1980, Tortorici 1981, Moussat et al. 1986), but no strike-slip stresses contemporaneous with extension are indicated. The Sant'Arcangelo basin developed later, at the end of the Pliocene or the beginning of the Pleistocene, in a compressional tectonic environment (N70° σ_1) which clearly differs from the Pliocene one.

Seismic profiles

Several seismic profiles of the Sant'Arcangelo basin were studied. A particularly representative line provides

Table 1. Palaeostress tensors computed from fault-slip analysis in the Sant'Arcangelo basin. Site localities are shown in Fig. 3. Age of fractured rocks. Type of event: S, strike-slip faulting; C, reverse faulting; E, normal faulting. N = number of faults used for tensor calculation. Stress axes: trend and plunge in degrees. $\Phi = (\sigma_2 - \sigma_3)/(\sigma_1 - \sigma_3)$. ANG = average angle between computed shear stress and observed slickenside lineation (in degrees)

| Site	Age of rocks	Type of event	N	Orientation of palaeostress			Φ	ANG
				σ_1	σ_2	σ_3		
1	Eocene	S	11	069 11	214 77	337 07	0.35	10
2	Miocene	S	09	058 15	284 68	152 15	0.17	12
3	Calabrian	C	26	255 03	163 33	350 57	0.20	13
4	early–middle Pliocene	S	14	245 01	338 76	155 14	0.16	16
4		E	15	118 66	284 23	016 05	0.44	14
5	Pliocene	S	23	021 06	140 77	290 11	0.28	09
7	Calabrian	C	06	251 27	348 12	099 60	0.53	07
8	Pliocene	E	21	031 77	231 13	140 04	0.32	11
10	early Pliocene	C	09	068 14	169 38	322 48	0.26	15
11	early Pliocene	S	05	257 23	013 47	150 35	0.20	20
13	Miocene	S	25	210 26	014 63	117 06	0.36	09
13		C	14	253 06	163 09	013 79	0.25	13
14	Pliocene	S	12	081 20	324 51	183 32	0.22	07
15	Pliocene	E	21	168 88	343 02	073 00	0.31	09
16	Pliocene	S	14	209 09	079 76	300 11	0.65	10
16		E	07	150 76	027 07	296 11	0.74	09
18	Calabrian	C	17	063 03	157 53	331 37	0.12	08
19	Calabrian	S	14	250 09	098 80	341 05	0.62	16
21	Pliocene	E	08	224 50	011 36	114 16	0.33	05
22	early–middle Pliocene	S	09	358 25	226 55	099 23	0.18	08
24	Pliocene	C	20	239 04	330 14	132 75	0.28	11
24		S	10	014 08	258 72	106 16	0.52	13
26	Serravallian	S	13	248 03	342 56	155 33	0.18	11
27	Serravallian	S	20	061 07	165 63	328 26	0.05	11
27		S	07	266 23	113 64	001 11	0.39	08
29	Burdigalian	S	10	226 01	320 80	136 10	0.48	12
33	Pliocene	E	05	045 72	193 15	285 09	0.53	13
33		S	10	024 01	292 66	114 24	0.21	11
33		C	34	062 03	153 12	318 77	0.04	09
34	Miocene	S	22	248 02	150 77	338 13	0.21	10
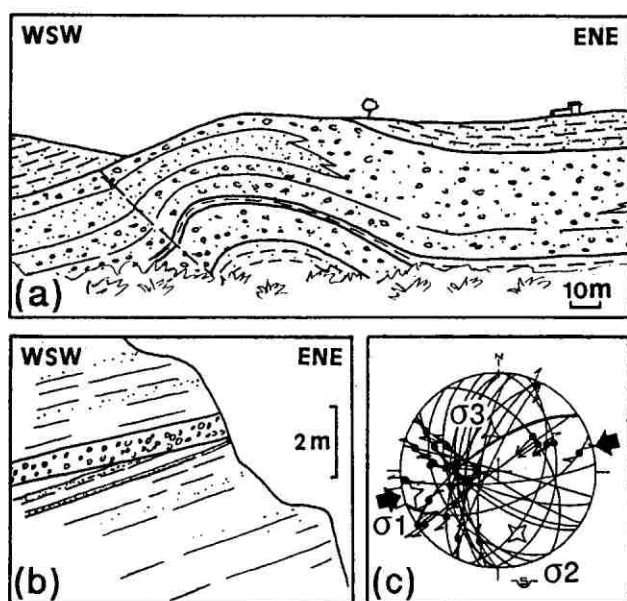
Fig. 6. Alianello anticline in the early Pleistocene sediments of the Sant'Arcangelo basin. (a) General view of the fold. (b) Angular unconformity in the western flank of the fold, just to the left of (a). (c) Schmidt diagram with the stress axes (N75° compression) computed from striated fault planes associated with the fold.

a cross-section through the entire Pleistocene basin (Figs. 3 and 8). As mentioned above, micropalaeontological analysis of marl samples collected along the trace of the seismic line assigns a Pleistocene age to the basal outcropping reflectors (east of the basin, Fig. 3). The seismic section (Fig. 8) shows a sedimentary sequence onlapping the southwestern border of the basin. Note that the presence of reverse faults indicates again the presence of compressional deformations (no evident normal fault being found). This Pleistocene sequence is tilted and eroded along the northeastern side of the basin. Since the upper sediments are gently deformed, we can assume that only minor deformation occurred in the basin at the termination of sedimentation. Moreover, if reflections represent isochrons, as envisaged by Vail et al. (1977), the profile reveals a migration of the depocentres from northeast to southwest, as a consequence of a progressive southwestward tilt of the whole basin. The geographic distribution of clays, sands and conglomerates (Fig. 3) fits very well with the syntectonic westward migration of depocenters within a regressive depositional sequence.

This interpretation in terms of Pleistocene syndepositional tilt of the Sant'Arcangelo basin is in agreement with the erosion of the Nocara–Valsinni anticline during its filling (Vezzani 1967), and also with the tilt of the lower Pleistocene sequence uncomformably overlain by a lower–middle Pleistocene terrace (Fig. 4). This hypothesis is also in agreement with our field observation of syn-depositional folding mentioned earlier (Fig. 6).

The model

Geological and palaeostress evidence indicates that the Pleistocene Sant'Arcangelo Basin developed under a compressional regime. The large-scale structure detected on seismic profiles (Fig. 8) resembles that of typical piggyback basins in the Po foredeep (Ori & Friend 1984), where tilt gradually decreases from lower reflections to upper ones. Borehole data suggest that, as in the Pliocene Po Valley piggyback basins (Pieri 1983), the Sant'Arcangelo basin has recorded progressive tilt during Pleistocene thrusting (Fig. 5). We thus consider that this syn-compressive basin is a piggyback basin. The migration of basin depocentres towards the southwest is explained in terms of deep-thrust emplacement.

To explain a migration of the depocentres in the direction opposite to that of thrusting, two hypotheses are possible (Roure et al. 1988): (1) the motion of a single deep-thrust along a single ramp (Fig. 9a); or (2) the development of an initial thrust ramp, later tilted together with the basin during the formation of a second external thrust (Fig. 9b). The two-thrust model of Fig. 9(b) agrees with the structural framework discussed herein (Fig. 5) much better. Two large Pleistocene piggyback basins exist in this area: Sant'Arcangelo and Metaponto (above the Metaponto thrust sheet) (Figs. 1 and 5). As in the model, these two basins are separated by a nappe anticline. We interpret the northern border of the Sant'Arcangelo basin (Fig. 3) as the lateral ramp of a thrust.

Summary

The Sant'Arcangelo basin, a large Pleistocene compressional structure, is bounded by strike-slip faults and folds (Fig. 3) corresponding to the formation of underlying lateral and frontal ramps (Fig. 5). This basin has a simple palaeostress history characterized by a single major N70° compression contemporaneous with its filling (Fig. 3). Remarkably, different structures including strike-slip faults, folds and reverse faults appear to correspond to a single mechanism: a N70° compression. Note that as a consequence of a nearly 20° anticlockwise block rotation evidenced in the Pliocene and Pleistocene sediments (Sagnotti 1992), the determined directions of compression may slightly differ from the initial ones. Nevertheless, structural and palaeostress studies confirm the existence of compressive regime contemporaneous with the development of this basin, which is interpreted as a typical recent piggyback basin.

THE OFANTO BASIN

The Ofanto basin (Fig. 1) is older (early–middle Pliocene, Vezzani 1968, Servizio Geologico d'Italia 1970, Bigi et al. 1992) than the Pleistocene Sant'Arcangelo basin, and reveals a polyphase evolution. It consequently provides an opportunity to study intramontane basin development during the whole Plio-Pleistocene.

Stratigraphy

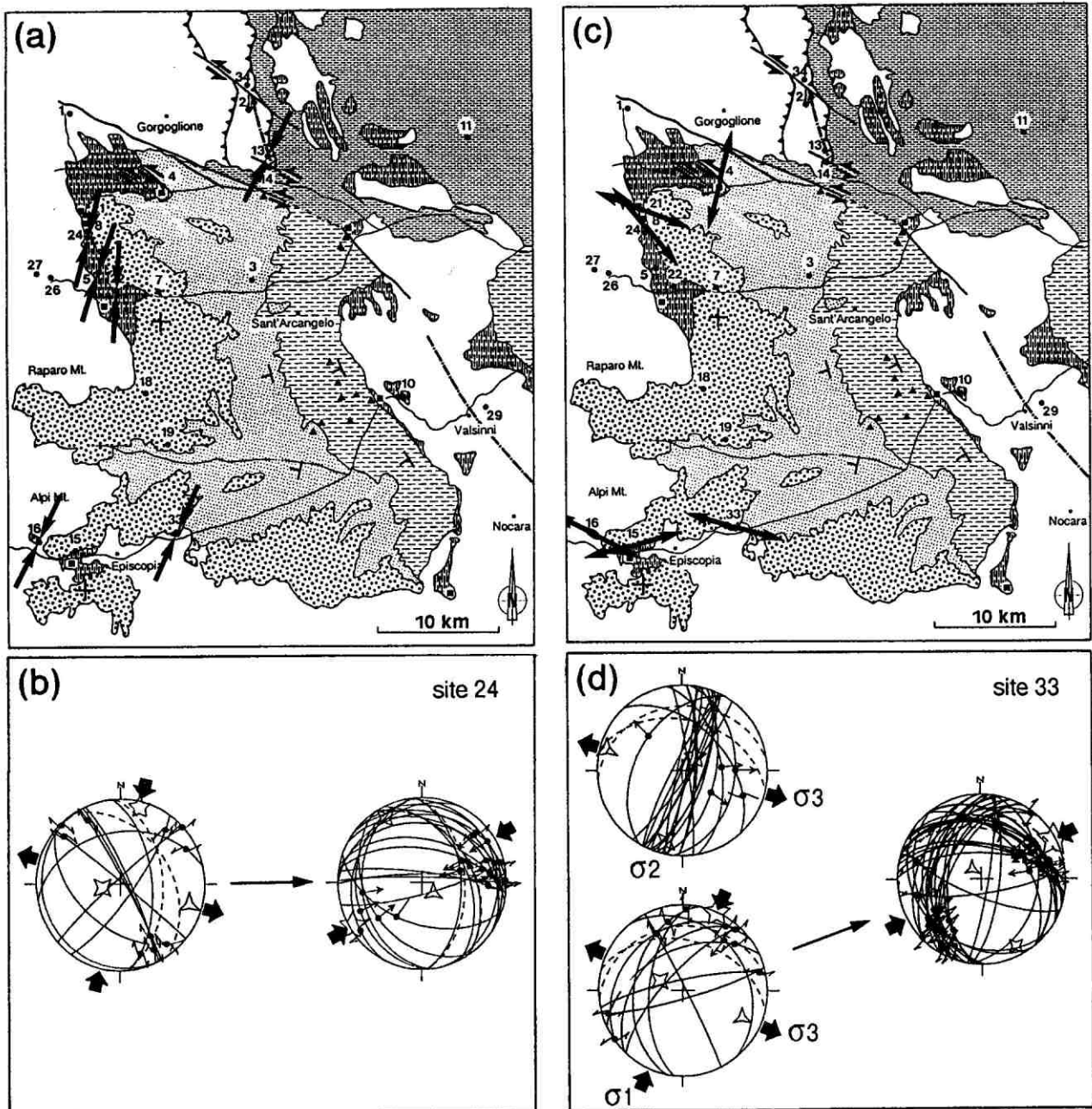The infill of this basin is mainly composed of marly clays and sandy clays (Fig. 10). As for the Sant'Arcan-

Fig. 7. Pliocene palaeostresses for Sant'Arcangelo basin; geology as Fig. 3. (a) Directions of compression from strike-slip faults. (b) Relative chronology between the N25° and N70° compressions in site 24. (c) Direction of extension from normal faults. (d) Example of site 33. Normal faults associated with tension gashes (first diagram) are sealed by Pleistocene formations; strike-slip deformations with the same trend of extension pre-date N70° compression.

gelo basin, there is an unusual areal distribution of the conglomerates. Conglomeratic sediments intercalated in the basin fill are only present in the northern portion of the basin, rather far from the carbonate source reliefs. Another conglomeratic unit, which constitutes the uppermost deposits of the basin fill, is present only in the eastern part of the basin.

Structures

As a first approximation, the Pliocene sediments are located within an elongate depression that trends E–W. These sediments overlie almost exclusively the 'argille varicolori' (Ogniben 1969), a part of the Lagonegro–Molise basinal sequence, often a chaotic tectonic

melange (Roure et al. 1991). The structural setting of the Ofanto basin substratum is thus unclear. Nevertheless, it is possible to identify a tectonic window of a radiolarite unit in the southeastern part of the basin (Fig. 10). To the east, early–middle Miocene flysch (Cocco et al. 1972) of the Lagonegro–Molise basinal sequence are folded and thrusted along the edge of the foredeep. The Vulture volcano (middle–late Pleistocene 0.74–0.59 Ma, La Volpe & Principe 1989) overlies these compressional structures and is thus more recent than them.

To the southwest, the Lagonegro–Molise units are overthrust by carbonates of the western platform (Casero et al. 1988), with possible local backthrusts (Mostardini & Merlini 1988) (Figs. 2 and 10) and local occurrences of normal faults.
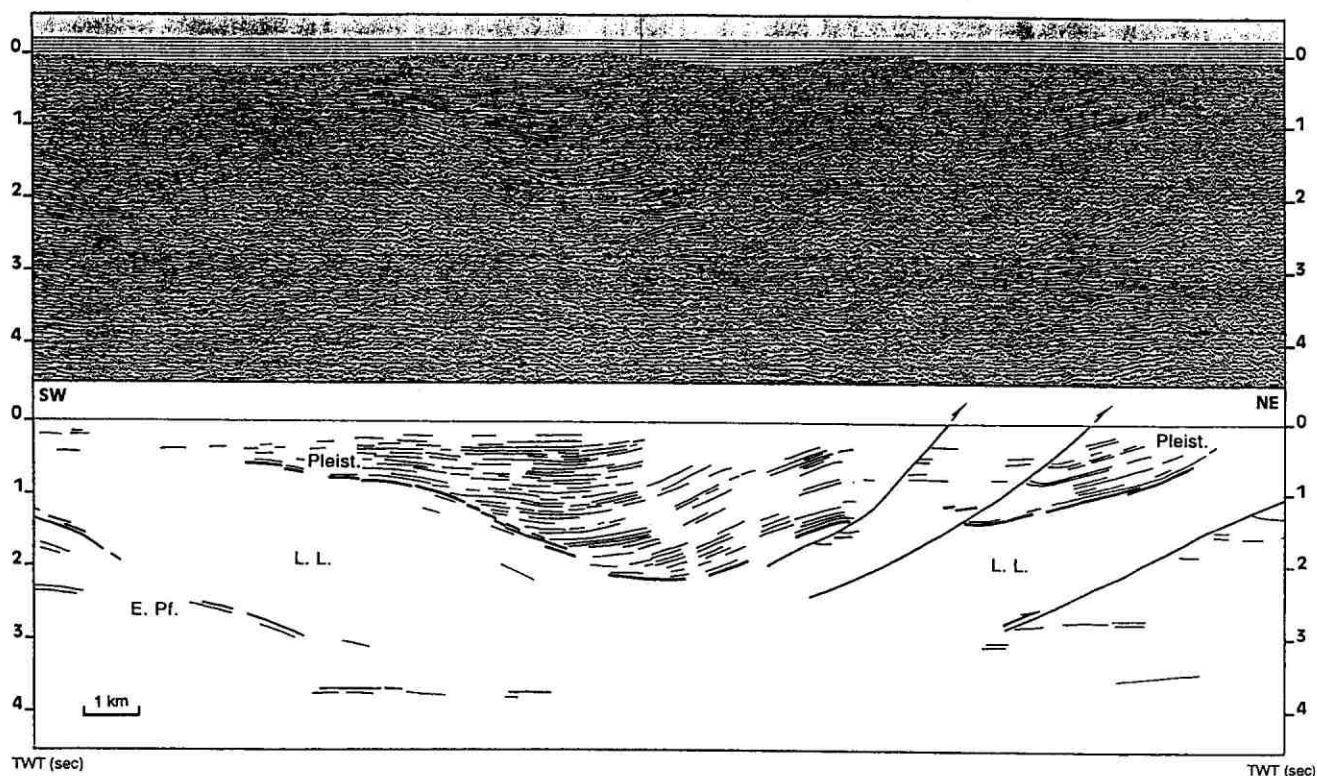
Fig. 8. Unmigrated seismic line and line drawing across the Sant'Arcangelo basin (see location in Fig. 3). Pleist., Pleistocene sediments; L.L., Lagonegro and Liguride pelagic units; E.Pf., carbonates of the eastern platform. Pleistocene sediments are tilted to the southwest and onlap older formations.
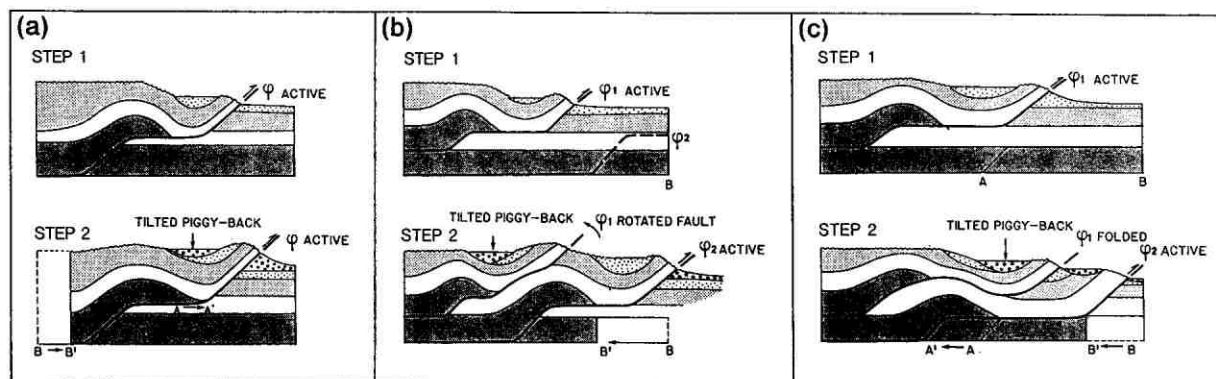

Fig. 9. Different models to explain a migration of the depocentres in the opposite direction of thrusting (a) (b), and in the direction of thrusting (c), in the case of two levels of décollement (Roure et al. 1988).

On the western border of the basin, Ortolani & Torre (1981) suggest the existence of a left-lateral strike-slip fault (Fig. 10). The geological map (Servizio Geologico d'Italia 1970) indicates the presence of normal faults near this fault. We shall demonstrate in a later subsection that the structure of the basin, although complex, is in fact simpler than expected from these scattered data.

Palaeostresses

Palaeostress reconstructions are made in the Ofanto basin and some adjacent outcrops (19 sites, 660 fault planes with slickenside lineations, Fig. 10). Both compression and extension are computed (Table 2 and Fig. 11). The directions of extension are scattered (Fig. 11a). In addition, several directions of extension are often determined in a given site (Table 2, sites 2, 23, 24 and 26). If such directions of extensions are contemporaneous, this implies that the ratio Φ (see Table 1) was close to zero (σ_2 nearly equal to σ_3). Since this extension was found exclusively in clays, or in conglomerates lying on the clays, we suspect that it resulted either from compaction or from gravity sliding. Alternatively, this extension could result from local perturbations near the large strike-slip fault noted by Ortolani & Torre (1981).

In contrast, conglomerates are affected mostly by compression. This compression is usually associated with a gentle tilt, but in some cases bedding planes are subvertical. The trends of compression are variable (Fig. 11b), but clearly correspond to several classes, with two major trends, N25° and N70° on average, and two minor ones, N110° and N170°. Relative chronology data based

on succession of slickenside lineations indicate that the N170° compression was followed by the N25° one, and then by the N70° direction (six observations in sites 24, 25, 31 and 32). The remaining compression, N110°, post-dates compression N170° (six observations in sites 32 and 34), but was identified as either older than compression N25° (one observation in site 2), or more recent (two observations in site 32). Because of these opposite relative chronologies, and because two compressions are perpendicular (N110° and N25°), we suggest that the N110° compression simply corresponds to a constrictive deformation during the N25° compression, and does not belong to a distinct tectonic event.

Locally, the relative chronology of tectonic events is confirmed by the relation of stress tensor with the bedding attitude. For example, in the site number 31, the bedding planes are subvertical and trending E–W (Fig. 12, diagram A). The reverse faults corresponding to the N–S compression (Fig. 12, diagram A') are presently tilted as well as the related computed stress axes (Fig. 12, diagram A). In contrast, the reverse faults corresponding to the more recent ENE–WSW compression (Fig. 12, diagram B) are found in their original position so that two of the computed stress axes remain horizontal.

Since the N70° compression is the most recent in the area considered and affects the Pleistocene rocks of the Vulture volcano (Fig. 10 and Table 2, site 30), it can be dated as Pleistocene, and correlated with the N70° Pleistocene compression of the Sant'Arcangelo basin. Two major directions of earlier compressions, a N170° followed by a N25°, are probably of Pliocene age (the latter being accompanied by a N110° transverse secondary compression).

We point out that evidence for extensional tectonism is scarce in this basin and does not correspond to major structures. Furthermore, the computed directions of extension are scattered and cannot be convincingly correlated with the structures in this E–W elongated basin. On the other hand, 75% of computed stress tensors correspond to compression, which was related to folding. Accordingly, the existence of distinct classes of σ_1 trends as well as of consistent relative chronologies suggest that the basin has been created by polyphase compression. Palaeostress reconstructions indicate that the Ofanto basin underwent polyphase compressional tectonism during the Pliocene, followed by Pleistocene compression similar to that identified in the Sant'Arcangelo basin.

Seismic profiles

Two seismic profiles of good quality illustrate the deep structure of the Ofanto basin. As for the Sant'Arcangelo basin, the profile A–A' (Figs. 10 and 13a) shows continuous reflections but in this case, no fault could be detected. The northeastern part of the line shows tilted reflections which are consistent with tilted beds observed in the field. As mentioned above, in some sites (e.g. site 31, Fig. 12), the tilted attitude of the stress axes indicates that the tilt of the beds (and the faults) results from tectonics. In the northeastern part of the line, the angle between the lower and upper reflectors is opened towards the southwest of the basin. This distribution indicates that this area was uplifted during sedimentation, as in a typical piggyback compressive basin. This structure is remarkably similar to those of the Sant'Ar-
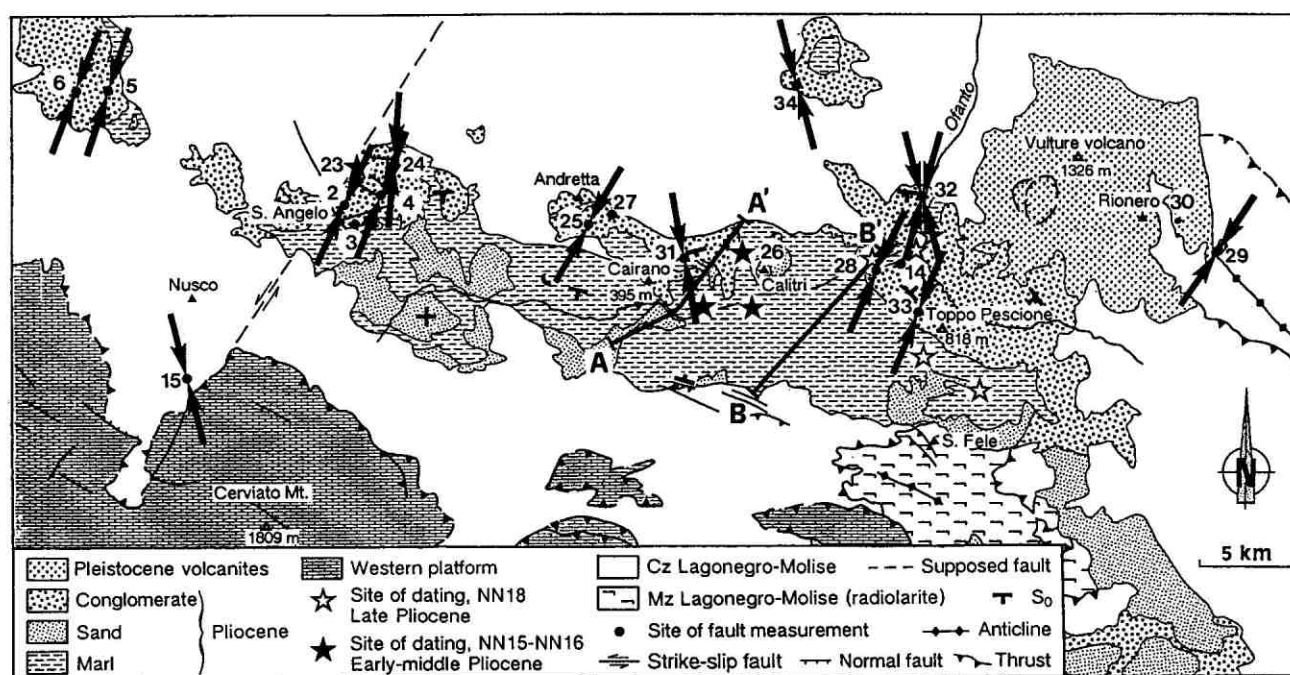

Fig. 10. Geological sketch of the Pliocene Ofanto basin (see location in Fig. 1) and sub-meridian directions of compression. A–A', B–B', traces of seismic sections of Fig. 13.

J. C. HIPPOLYTE, J. ANGELIER, F. ROURE and P. CASERO

Table 2. Palaeostress tensors computed from fault-slip analysis in the Ofanto basin. Site localities shown in Fig. 10. Same legend as Table 1

Site	Age of rocks	Type of event	N	Orientation of palaeostress			Φ	ANG
				σ_1	σ_2	σ_3		
2	early–middle Pliocene	E	23	016 78	279 02	188 12	0.35	12
2		E	19	302 84	033 01	123 06	0.34	11
2		S	09	114 11	007 57	211 31	0.16	11
2		C	04	025 05	286 60	118 29	0.19	03
3	early–middle Pliocene	S	08	067 15	271 74	159 06	0.75	13
4	early–middle Pliocene	S	07	077 15	253 75	346 01	0.44	12
4		C	06	022 05	113 18	276 71	0.40	16
5	early middle Pliocene	C	19	249 06	154 40	345 49	0.18	08
5		C	07	198 05	288 02	044 85	0.37	04
5		S	09	285 09	040 69	191 18	0.13	07
6	early–middle Pliocene	C	17	014 05	105 11	261 78	0.44	12
6		S	15	250 07	063 83	160 01	0.27	14
6		C	13	210 01	119 37	301 53	0.05	11
14	late Pliocene	S	06	262 15	094 74	353 03	0.75	13
15	Cretaceous	S	14	164 40	347 50	255 01	0.77	04
23	early–middle Pliocene	E	20	218 72	048 18	317 03	0.24	07
23		E	24	214 71	101 07	009 17	0.18	07
23		E	23	271 78	147 07	056 10	0.46	06
24	early–middle Pliocene	E	22	216 74	338 09	070 13	0.39	10
24		E	11	134 71	234 15	007 12	0.53	12
24		C	10	186 18	286 27	066 57	0.38	06
24		S	08	252 24	112 60	350 17	0.20	15
25	early–middle Pliocene	C	15	031 07	300 01	200 82	0.18	11
25		S	13	076 16	184 48	334 37	0.10	11
26	early–middle Pliocene	E	17	041 75	239 14	148 04	0.35	10
26		E	10	332 72	105 13	198 13	0.44	15
26		E	21	139 71	010 12	277 15	0.29	16
26		S	14	073 21	239 68	342 05	0.19	12
27	early–middle Pliocene	C	21	113 07	020 21	221 68	0.42	10
28	late Pliocene	C	11	023 12	293 01	201 78	0.05	11
29	Mio-Pliocene	S	12	216 11	036 79	126 01	0.12	14
29		C	18	212 01	122 03	325 87	0.46	08
30	Pleistocene	E	24	077 75	237 14	328 05	0.50	15
30		S	12	054 18	248 71	146 04	0.35	11
31	early–middle Pliocene	C	14	063 05	153 01	247 85	0.34	09
31		S	21	254 07	122 79	345 08	0.40	14
31		C	14	180 56	085 03	353 34	0.20	15
32	early–middle Pliocene	S	24	162 17	025 68	256 14	0.47	14
32		C	10	198 06	107 08	324 80	0.49	09
32		C	43	115 03	205 01	323 87	0.24	09
33	late Pliocene	C	10	022 13	115 12	247 73	0.37	10
34	early–middle Pliocene	C	11	346 07	079 24	241 64	0.13	08
34		C	17	292 01	202 09	024 81	0.32	11
34		C	18	063 11	160 30	315 58	0.14	09

cangelo basin (Fig. 8), with a backward migration of the depocentres.

In the profile B–B' (Fig. 10 and 13b), the uppermost reflectors are tilted northeastwards. However, as for the A–A' section, the wedging of the upper sediments is evident in the northeastern part of the basin.

Both profiles show reflectors forming an angle opened towards the southwest of the basin, indicating that the basin was tilted mostly southwards during sedimentation. In the case of section B–B' (Fig. 13b), after a first syn-depositional southward tilt (Fig. 13a), the basin was tilted northeastwards and eroded in its southwestern part (Fig. 14). Note that the southwestern part of the profile B–B' is located close to a nappe anticline outlined by the radiolarite inlier of Fig. 10, and to NW–SE-trending reverse faults, which are oblique to the basin axis. We interpret this local northeastward tilt of the Pliocene sediments as a result of the formation of the nappe anticline in the southeastern part of the basin.

The model

Structural and palaeostress studies show that the Ofanto basin is of compressive piggyback origin. This basin has undergone a polyphase history characterized by two successive tilts. During a first stage, the basin was created due to a NNW–SSE compression (Fig. 15a); its present-day axis trends E–W, still approximately perpendicular to this early NNW–SSE compression. The depocentres migrated backwards (southwards), in consistency with sedimentary filling controlled by tilt during tectonic compression. This tilt is related to the thrusting activity of two ramps and one flat (Fig. 9a). In contrast with the Sant'Arcangelo–Metaponto couple of basins, there is a single Ofanto basin, whose development is related to the continuous activity of a single thrust. During thrusting, earlier deposits are tilted while passing over the ramp. The active depocentre was thus continuously present at the rear of the thrust ramp (Fig.
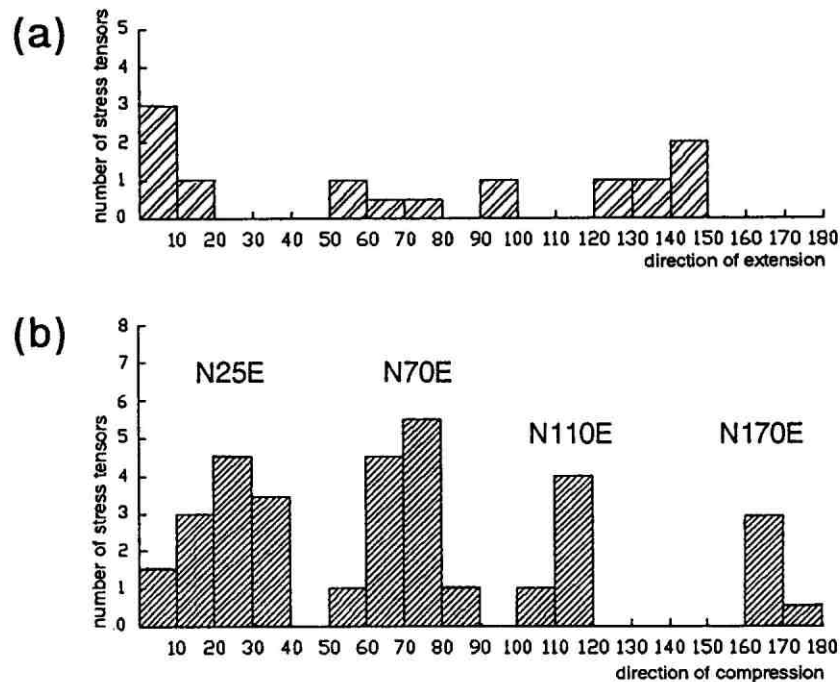
Fig. 11. Histograms of computed directions of extension and compression in Plio-Quaternary sediments in and around the Ofanto basin. (a) Directions of extension (normal faulting). (b) Directions of compression (strike-slip or reverse faulting).

9a). From this model, we can infer the existence of ramps and flats trending E–W in the units underlying the piggyback structure (Fig. 15a).

At the second stage, the thrust activity created a nappe anticline in the eastern portion of the Ofanto basin (see the radiolarite inlier of Fig. 10). This anticline induced the forward (northeastward) tilt of the eastern portion of the basin (Fig. 13b). This second tilt can be explained by the activity of an oblique thrust, with the creation of a ramp located west of the first depocentre (Figs. 9c and 15b). Based on this model, we infer the presence of a second depocentre, contemporaneous to this second (northeastward) tilt. To check this hypothesis, new nannoplankton dating was carried out: in the whole basin, the zones NN15 and NN16 of the early–middle Pliocene were identified (presence of *Discoaster surculus, D. asymmetricus, D. tamalis, Reticulofenestra pseudoumbilica* in sites of Fig. 10). The zone NN18 of

the late Pliocene age (presence of *Helicosphaera sellii, Pseudoemiliania lacunosa, Gephyrocapsa* sp., *Cyclicargolithus macintyrei, Discoaster brouweri*) was found only in the eastern part of the basin (Fig. 10), just below the uppermost conglomeratic formation. This formation is more recent than others in the basin, but is absent in profile B–B' (Fig. 13b) which followed the valley far below the conglomerates.

We conclude that two different sequences are present in the Ofanto basin. The first one, early–middle Pliocene in age (zones NN15–NN16), constitutes most of the basin fill and is clearly identifiable in seismic profiles. The second one, late Pliocene in age (zone NN18), is only present in the eastern part of the basin (Fig. 15b), near the nappe anticline (Fig. 10). As a consequence, the first stage of formation of this basin (Fig. 15a) is dated as early–middle Pliocene. The tilt of the basin occurred backwards and was progressively recorded by
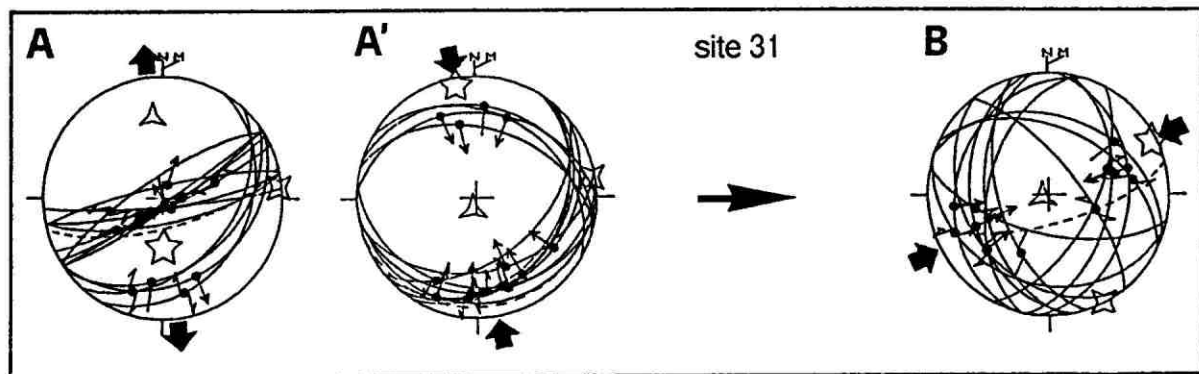

Fig. 12. Example of relative chronology revealed by bedding tilt. Diagram A, present attitude of faults and bedding plane (broken line); diagram A', diagram A after backtilting; note that all faults are reverse; diagram B, present attitude of the WSW–ENE compression (untilted). Faults of the NNW–SSE compression and bedding planes were tilted before WSW–ENE compression.
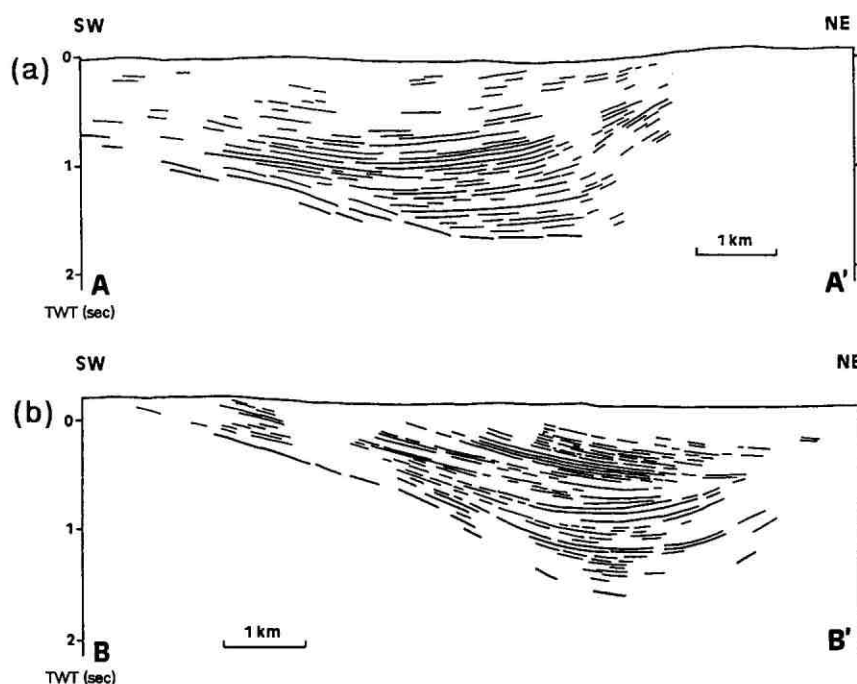
Fig. 13. Line drawings of the Ofanto basin from seismic profiles. (a) section A–A'; (b) section B–B' of Fig. 10.

the sedimentation (Figs. 9a and 13a). The second stage, late Pliocene in age, was contemporaneous with the oldest compression found in the late Pliocene sediments, trending NNE–SSW (Fig. 15b). This event was probably accompanied by constrictive deformation (i.e. the secondary WNW–ESE compression discussed earlier). According to this model, we infer the existence of NW–SE-trending ramps, particularly beneath the nappe anticline which is at the intersection of two ramps with different trends (compare Figs. 10 and 15).

The existence of two ramp trends under the Ofanto basin (Fig. 15) is not inferred from our analysis alone, but is also suggested by subsurface structure. A map (Fig. 16, Casero et al. 1991, Roure et al. 1991), based on seismic profiles and borehole data, shows that the ramps deduced from the geometry of the Ofanto piggyback basin are located in the carbonates of the eastern platform, buried beneath the basinal units. The NW–SE-trending ramp lies below the E–W ramp, which suggests that it is the most recent. This relative chronology is consistent with that independently reconstructed at the

Fig. 14. A–A' section (Fig. 13a) tilted as the B–B' section (Fig. 13b).

surface (between the NW–SE- and E–W-trending structures, Fig. 15) bringing further confirmation that the evolution of this basin reflects thrust activity.

The last ENE–WSW compression, of Pleistocene age, and identical to that of the Sant'Arcangelo basin, did not induce large structures in this area. However, it resulted in the Pleistocene thrusting of the front of the chain. This has been documented on seismic profiles (Casero et al. 1991) and also in the field (Hippolyte 1992).

SYNTHESIS AND CONCLUSIONS

In the Italian Sant'Arcangelo and Ofanto basins, the major structures are compressional and include folds, thrusts, strike-slip and reverse faults. In the Pleistocene part of the Sant'Arcangelo basin, the whole deformation is compressive and clearly syn-depositional. In the Pliocene basin fills (Sant'Arcangelo and Ofanto), extension was also found. In the Ofanto basin, seismic profiles did not reveal normal faults but only tilted sediments and depocentres migrations. As extension was principally found in clay sediments, we relate it to sliding or compaction rather than to genuine tectonic activity. In the Sant'Arcangelo area, contemporaneous strike-slip and extensional stresses may reflect the spatial transition from the compressional Ofanto basin to the extensional Calabria during the Pliocene.

We show that most of the stress tensors computed are compressional and adequately explain the major structures. In the two basins, syn-depositional tectonics resulted in the formation of stratigraphic wedges. The angle between reflectors is usually opened in the direction of recorded tilt. In all cases, it is possible to correlate these tilts with development of nappe anticlines near the surface, and to ramp–thrust activity underneath.
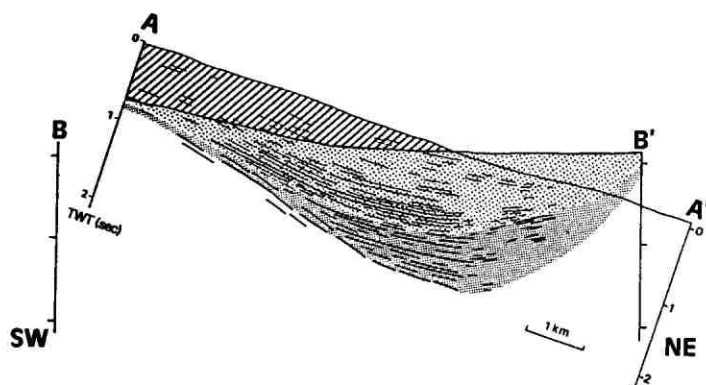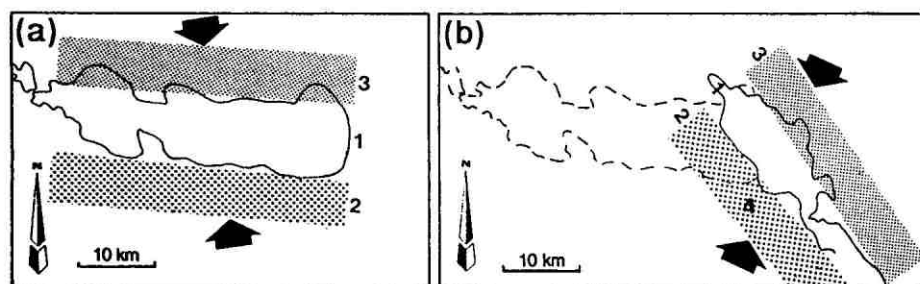
Fig. 15. Evolution of the Ofanto basin. (a) Early–middle Pliocene, formation and filling of the basin upon a thrust flat (1) limited by a deep ramp (2) and a shallow one (3) (see Fig. 9a). Compression is N170°. (b) late Pliocene, filling of the eastern part of the basin and local tilt of previous depocentre (see Fig. 9c). Compression trends N25°. Compare with the subsurface map of Fig. 16.

Clearly, the Pleistocene Sant'Arcangelo basin and the Ofanto basin can be interpreted as piggyback because they formed during compression on moving thrust sheets. The Sant'Arcangelo basin is a monophase piggyback basin; in contrast, the Ofanto basin underwent two compressional piggyback events.

These Plio-Quaternary piggyback basins recorded the deformation of the deeply buried eastern platform underneath the basinal units (Fig. 16). In particular, the Ofanto basin was created during the formation of the overthrust belt. Thrusts created in this structure propagated across the already deformed allochtonous basinal units along ramp and flat geometries (Figs. 2 and 5). This second deformation of the basinal units explains the common association of the piggyback basins with nappe anticlines. Superposed tectonics and the presence of multiple décollement levels (Fig. 9) contrast with those of the Po plain piggyback basins.

The study of such piggyback basins helps to constrain the geometric interpretation of subsurface structures. This is particularly important as they are often poorly imaged in seismic profiles in the southern Apennines, owing to the presence of tectonic melange units. This study also allows accurate dating of thrust activity (Fig. 16), deformation of mountain belt and compressional events.
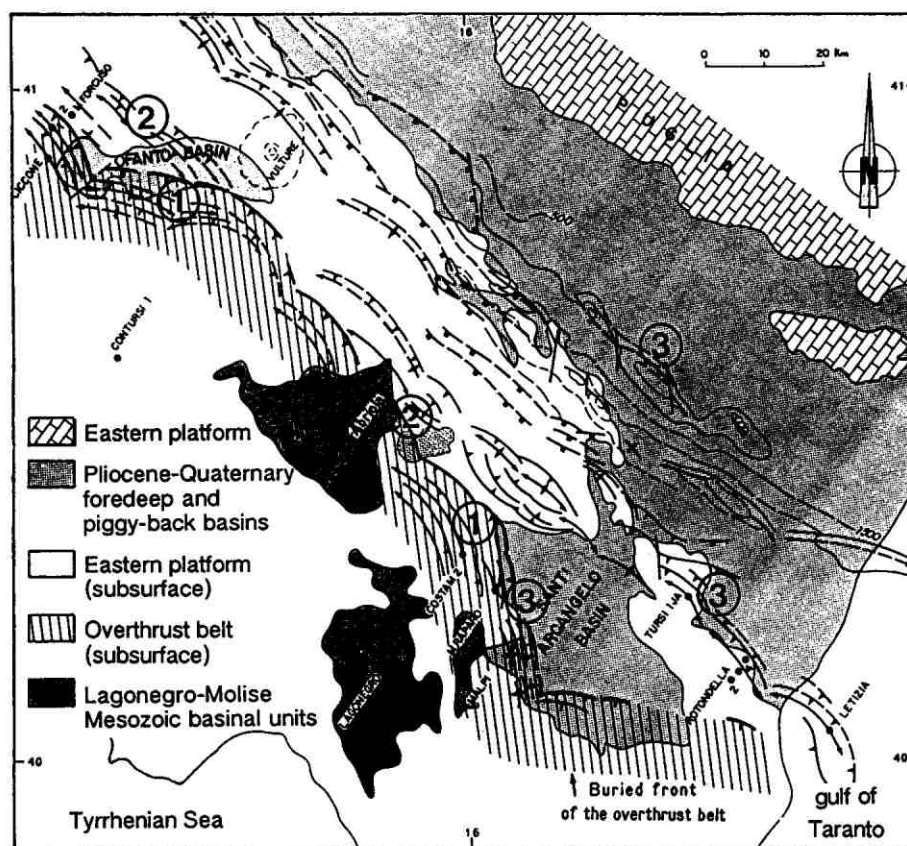

Fig. 16. Relation between subsurface structures (para-autochtonous of the eastern platform) and the piggyback basins (from Roure et al. 1991, modified). Piggyback dating allows dating of thrust plane activity: 1, early–middle Pliocene (nannoplankton zones NN15–NN16); 2, late Pliocene (zone NN18); 3, late Pliocene–early Pleistocene. Thrusting in the eastern platform is younger northeastwards. Outcrops of Lagonegro–Molise Mesozoic units outline the major nappe anticlines. Piggyback basins are mainly located northeast of the overthrust belt.

The southern Apennines region is presently mostly in extension, contemporaneous with isostatic rebound, whereas it was previously characterized by compression. Compression was contemporaneous with sedimentation, which demonstrates that it did not occur as a brief isolated compressive event as commonly accepted (e.g. Moussat 1983, Patacca & Scandone 1987). During the early Pleistocene (zone NN19), the mountain belt underwent WSW–ENE compression which created the piggyback basins of the south (Sant'Arcangelo and Metaponto, Figs. 1 and 16). During the Pliocene (zones NN15–NN16), and probably earlier, NNE–SSW- to NNW–SSE-trending compressions dominated (Figs. 7a and 10).

REFERENCES

Anderson, H. & Jackson, J. 1987. The deep seismicity of the Tyrrhenian sea. *Geophys. J. R. astr. Soc.* **91**, 613–637.

Angelier, J. 1990. Inversion of field data in fault tectonics to obtain the regional stress—III. A new rapid direct inversion method by analytical means. *Geophys. J. Int.* **103**, 363–376.

Angelier, J. & Bergerat, F. 1983. Systèmes de contraintes et extension intracontinentale. *Bull. Centres Rech. Explor.-Prod. Elf-Aquitaine* **7**, 137–147.

Balduzzi, A., Casnedi, R., Crescenti, U., Mostardini, F. & Tonna, M. 1982. Il Plio-Pleistocene del sottosuolo del Bacino Lucano (Avanfossa Appenninica). *Geol. Romana* **21**, 89–111.

Bigi, G., Cosentino, D., Parotto, M., Sartori, R. & Scandone P. 1992. Structural model of Italy, scale 1:500.000, sheet No. 4, C.N.R.

Boccaletti, M., Horvath, F., Loddo, M., Mongelli, F. & Stegena, L. 1976. The Tyrrhenian and Pannonian Basins: A comparison of two Mediterranean Interarc Basins. *Tectonophysics* **35**, 45–69.

Bousquet, J. C. 1973. La tectonique récente de l'Apennin Calabrolucanien dans son cadre géologique et géophysique. *Geol. Romana* **12**, 1–103.

Bousquet, J. C., Carveni, P., Lanzafame, P., Philip, H. & Tortorici, L. 1980. La distension pléistocène sur le bord oriental du Détroit de Messine: Analogies entre les résultats microtectoniques et le mécanisme au foyer du seisme de 1908. *Bull. Soc. géol. Fr.* **7**, 327–336.

Caldara, M., Loiacono, F., Morlotti, E., Pieri, P. & Sabato, L. 1988. Caratteri geologici e paleoambientali dei depositi Plio–Pleistocenici del bacino di S. Arcangelo (parte setentrionale); Italia meridionale. In: *L'Appennino Campano-lucano nel quadro geologico dell'Italia Meridionale.* Atti del 74° Congresso Soc. Geol. It., Sorrento 13–17 settembre 1988 (edited by Società Geologica Italiana). De Frede, Napoli. B, 51–58.

Casero, P., Roure, F., Moretti, I., Muller, C., Sage, L. & Vially, R. 1988. Evoluzione geodinamica neogenica dell'Appennino Meridionale. In: *L'Appennino Campano-lucano nel quadro geologico dell'Italia Meridionale.* Atti del 74° Congresso Soc. Geol. It., Sorrento 13–17 settembre 1988 (edited by Società Geologica Italiana). De Frede, Napoli. Relazioni, 59–66.

Casero, P., Roure, F. & Vially, R. 1991. Tectonic framework and petroleum potential of the Southern Apennines. In: *Generation Accumulation and Production of Europe's Hydrocarbons* (edited by M. Spencer). *Spec. Publ. Eur. Ass. Petrol. Geoscient.* **1**, 1–23, 381–387.

Castellarin, A. & Vai, G. B. 1986. South Alpine versus Po Plain Apenninic arcs. In: *The Origin of Arcs* (edited by Wezel, F. C.). Elsevier, Amsterdam, 253–280.

Cocco, E., Cravero, E., Ortolani, F., Pescatore, T., Russo, M., Sgrosso, I. & Torre, M. 1972. Les faciès sédimentaires Miocènes du bassin Irpinien (Italie Méridionale). *Atti. Acc. Pont.* **21**.

D'Argenio, B., Pescatore, T. & Scandone, P. 1975. Structural pattern of the Campania–Lucania Apennines. In: *Structural Model of Italy* (edited by Ogniben, L., Parotto, M. & Praturlon, A.). *Quad. Ric. Sci.* **90**, 313–327.

Fesce, A. M. 1987. Deformazioni compresive neogeniche nei conglomerati messiniani del bacino sinclinalico Giaggiolo-Cella (Forli). *Mem. Soc. geol. It.* **39**, 345–358.

Gars, G. 1983. Etude sismotectonique en Méditerranée Centrale et Orientale: I. La tectonique de l'Apennin Méridional et le séisme (2 nov. 1980) de l'Irpinia (Italie). II. Les failles activées par les séismes (fev.-Mars 81) de Corinthie (Grèce). Unpublished Ph.D. thesis, Paris-Sud Orsay.

Gasparini, C., Iannaccone, G., Scandone, P. & Scarpa, R. 1982. Seismotectonics of the Calabrian Arc. *Tectonophysics* **84**, 267–286.

Grandjacquet, C. & Mascle, G. 1978. The structure of the Ionian sea Sicily and Calabria-Lucania. In: *The Ocean Basins and Margins, Volume 4B* (edited by Nairn, A. E. M., Kanes, W. H. & Stehli, F. G.). Plenum Press, New York, 257–329.

Ghisetti, F. 1979. Evoluzione neotettonica dei principali sistemi di faglie della Calabria Centrale. *Boll. Soc. geol. It.* **98**, 387–430.

Haccard, D., Lorenz, C. & Grandjacquet, C. 1972. Essai sur l'évolution tectogénétique de la liaison Alpes–Apennines (de la Ligurie à la Calabre). *Mem. Soc. geol. It.* **11**, 309–341.

Hippolyte, J.-C. 1992. Tectonique de l'Apennin méridional: structures et paleocontraintes d'un prisme d'accrétion continental. Unpublished Ph.D. thesis, Université P. et M. Curie, Paris.

Hippolyte, J.-C., Angelier, J. & Roure, F. 1992. Les permutations d'axes de contraintes: exemples dans des terrains quaternaires du sud de l'Apennin (Italie). *C. r. Acad. Sci., Paris* **315**, 89–95.

Ippolito, F., D'Argenio, B., Pescatore, T. & Scandone, P. 1975. Structural–stratigraphic units and tectonic framework of Southern Apennine. In: *Geology of Italy, II* (edited by Squyres, C. H.). Earth Science Soc. of the Libyan Arab Republic, Tripoli, 317–328.

Kastens, K. A., Mascle, J., Auroux, C. *et al.* 1987. *Proc. Init. Reps. (Pt. A) ODP* **107**, 1013 p.

La Volpe, L. & Principe, C. 1989. Stratigrafia e storia eruttiva del Monte Vulture: Revisione ed aggiornamenti. *Bollettino GNV* **1989-2**, 889–902.

Mostardini, F. & Merlini, S. 1988. Appennino Centro-Meridionale: Sezioni Geologiche e proposta di modello strutturale. *Mem. Soc. geol. It.* **35**, 177–202.

Moussat, E. 1983. Evolution de la Mer Tyrrhénienne Centrale et Orientale et de ses marges Septentrionales en relation avec la néotectonique dans l'Arc Calabrais. Unpublished Ph.D. thesis, Université P. et M. Curie, Paris.

Moussat, E., Angelier, J., Mascle, G. & Rehault J. P. 1986. L'ouverture de la mer Tyrrhénienne et la tectonique de faille néogène quaternaire en Calabre. *Giorn. Geol.* **48**, 63–75.

Ogniben, L. 1969. Schema geologico introduttivo alla geologia del confine Calabro Lucano. *Mem. Soc. geol. It.* **8**, 453–763.

Ori, G. G. & Friend, P. F. 1984. Sedimentary basins formed and carried piggyback on active thrust sheets. *Geology* **12**, 475–478.

Ortolani, F. & Torre, M. 1981. Guida all'escursione nell'area interessata dal terremoto del 23-11-1980. *Rend. Soc. geol. It.* **4**, 173–214.

Patacca, E. & Scandone, P. 1987. Post-Tortonian mountain building in the Apennines: the role of the passive sinking of a relic lithospheric slab. In: *The Lithosphere in Italy. Advances in Earth Sciences Research* (edited by Boriani, A., Bonafede, M., Piccardo, G. B. & Vai, G. B.). *Rend. Acc. Naz. Lincei* **80**, 157–176.

Pieri, M. 1983. Three seismic profiles through the Po Plain. In: *Seismic Expression of Structural Styles. A Picture and Work Atlas* (edited by Bally, A. W.). *Am. Ass. Petrol. Geol.* **3**, 341.8–341.26.

Ricci Lucchi, F. 1986. The Oligocene to Recent foreland basins of the northern Apennines. *Spec. Publ. Int. Ass. Sediment.* **8**, 105–139.

Ritsema, A. R. 1979. Active or passive subduction at the Calabrian Arc. *Geol. Minjb.* **58**, 127–134.

Roure, F., Casero, P. & Vially, R. 1988. Evolutive geometry of ramps and piggyback basins in the Bradanic trough. In: *L'Appennino Campano-lucano nel quadro geologico dell'Italia Meridionale.* Atti del 74° Congresso Soc. Geol. It. Sorrento 13–17 settembre 1988 (edited by Società Geologica Italiana). De Frede, Napoli. B, 360–363.

Roure, F., Casero, P. & Vially, R. 1991. Growth processes and melange formation in the southern Apennines accretionary wedge. *Earth Planet. Sci. Lett.* **102**, 395–412.

Sagnotti, L. 1992. Paleomagnetic evidence for a Pleistocene counterclockwise rotation of the Sant'Arcangelo Basin southern Italy. *Geophys. Res. Lett.* **19**, 135–138.

Servizio Geologico d'Italia, 1970. Carta geologica d'Italia, foglio 186, S. Angelo de'Lombardi 1:100.000 Redini, R. (Coord.).

Tortorici, L. 1981. Analisi degli deformazioni fragili dei sedimenti post orogeni della Calabria Settentrionale. *Boll. Soc. geol. It.* **4**, 1–18.

Vail, P., Mitchum, R. & Thompson, S. 1977. Seismic stratigraphy and global changes of sea level. *Mem. Am. Ass. Petrol. Geol.* **26**, 49–212.

Vezzani, L. 1967. Il Bacino Plio-Pleistocenico di San Arcangelo (Lucania). *Atti Acc. Gioenia Sc. Nat. Catania S6*, **18**, Suppl. Sc. Geol., 207–227.

Vezzani, L. 1968. Stratigrafia dei terreni infra-mesopliocenice di Ruvo del Monte (Potenza). *Boll. Acc. Gioenia Sc. Nat. Catania* **9**, 3–41.

Vezzani, L. 1975. Lithostratigraphic complexes and evidence for tectonic phases in the Molise–Puglia–Lucania Apennines. In: *Structural Model of Italy* (edited by Ogniben, L., Parotto, M. & Praturlon, A.). *Quad. Ric. Sci.* **90**, 329–363.

Zoetemeijer, R., Sassi, W., Roure, F. & Cloetingh S. 1992. Stratigraphic and kinematic modeling of thrust evolution, northern Apennines, Italy. *Geology* **20**, 1035–1038.